Measurement of Defect-Mediated Diffusion: The Case of Silicon Self-Diffusion

Ramakrishnan Vaidyanathan, Michael Y. L. Jung, Richard D. Braatz, and E. G. Seebauer
Dept. of Chemical Engineering, University of Illinois, Urbana, IL 61801

DOI 10.1002/aic.10587
Published online September 19, 2005 in Wiley InterScience (www.interscience.wiley.com).

In many solids, diffusion of foreign atoms takes place primarily through highly mobile intermediate species that periodically exchange with atoms in the crystalline lattice. A method is developed for determining key diffusion parameters via the short-time decay of an initial step concentration profile. This method takes advantage of the relative ease with which step concentration profiles can be fabricated by thin film deposition, and in the limit of very short times provides particularly simple analytical means for obtaining parameters connected to diffusion length and defect formation. Application of the method to isotopic heterostructures of silicon shows that under the ultrahigh vacuum conditions of the experiment, interstitial atoms mediate self-diffusion. © 2005 American Institute of Chemical Engineers *AIChE J,* 52: 366–370, 2006

Introduction

Diffusion of foreign atoms in solids has been studied extensively to understand the governing mechanisms and, in the case of semiconductors, to facilitate improvements in device fabrication. In many cases such as silicon, studies of dopant diffusion[6,8,10] and isotopic self-diffusion[6,13] have suggested that migration takes place primarily through highly mobile intermediate species (such as interstitial atoms) that periodically exchange with atoms in the crystalline lattice. Experimental methods for such studies often measure the decay of an artificially created concentration profile. The initial shapes can be delta functions[3] or steps.[1,14] For long-time diffusion, Fick's Second Law with a constant- diffusion coefficient often offers a satisfactory framework for data analysis. Experimental profiles are usually fitted with Gaussian or error-function forms in the respective cases of delta functions or steps.

However, Cowern et al[3] have shown that for short diffusion times, the dynamics of intermediate-species creation, motion and annihilation can no longer be neglected. These workers constructed a suitable mathematical description for the case of an initial delta-function profile,[3] and applied the resulting expressions to boron diffusing in silicon. The description provides two parameters describing motion and exchange of the intermediate species instead of a single composite diffusion coefficient, thereby offering more insight into diffusion mechanisms. For sufficiently short times, profiles decay with "exponential tails" that provide an unmistakable signature of diffusion via a fast-moving intermediate species. The exponential tails simplify data analysis and decrease the susceptibility to errors in fitting the two parameters.

Unfortunately, the creation of delta-function initial profiles often requires fairly sophisticated fabrication techniques that require precise on-off control of the foreign atom concentration. Step functions tend to be easier to create by standard thin-film deposition techniques, but to our knowledge the advantages of short-time measurements have not been exploited for initial step profiles. This article derives the required mathematical framework.

Furthermore, the framework is applied to experimental data for the self-diffusion of the ^{30}Si isotope into a ^{28}Si matrix. The mechanism for Si self-diffusion has generated much controversy over many years. Older literature[7,8,11] has suggested that self-interstitials mediate diffusion at high temperatures, while vacancies dominate at lower ones. More recent results argue for the predominance of interstitials at all temperatures,[1] or for a combination of the mechanisms with very similar temperature dependences.[13] Shape analysis of the present results shows that interstitial atoms carry the primary diffusion flux in Si self-diffusion under the conditions of the experiment, as opposed to vacancies.

Correspondence concerning this article should be addressed to E. G. Seebauer at eseebaue@uiuc.edu.

© 2005 American Institute of Chemical Engineers

Table 1. Rate Expressions for Defect/Foreign Atom Pairing Mechanisms

Type of Reaction	Stoichiometry	Generation		Annihilation	
		Rate	First-Order Rate Constant	Rate	First-Order Rate Constant
Interstitial (kick-out)	$S + I \Leftrightarrow M + H$	$k_{gen}C_I C_S$	$k_{gen}C_I$	$k_{ann}C_H C_M$	$k_{ann}C_H$
Interstitial (dissociation)	$S \Leftrightarrow M + V$	$K_{gen}C_S$	K_{gen}	$k_{ann}C_V C_M$	$k_{ann}C_V$
Vacancy pair (combination)	$S + V \Leftrightarrow M$	$k_{gen}C_V C_S$	$k_{gen}C_V$	$K_{ann}C_M$	K_{ann}
Vacancy pair (dissociation)	$S \Leftrightarrow M + I$	$K_{gen}C_S$	K_{gen}	$k_{ann}C_I C_M$	$k_{ann}C_I$

Theory

The foreign atoms under consideration are typically dopants or unintentional impurities present in low concentrations (< 1%), but isotopic variants of the host can be treated in the same way. Diffusion of such species is often mediated by point defects such as interstitials and vacancies,[12] which can migrate alone or bond to foreign atoms to form mobile defect-dopant pairs.[7, 8, 11] Cowern et al. [4] have enumerated four ways in which foreign atoms in substitutional sites (S) can enter into highly mobile states (M) by interaction with host interstitials (I) or vacancies (V). Corresponding rate expressions can be written as summarized in Table 1, where C_M, C_S, C_I, C_V, and C_H, respectively, represent the concentrations of foreign mobile-state species, foreign substitutional atoms, host interstitials, vacancies, and host lattice atoms (H). Similar rate expressions can also be written for mobile species annihilation, also shown in Table 1. The parameters K and k respectively denote first- and second-order rate constants. In all cases, the second-order expressions can be written in pseudo first-order form by recognizing that the total concentration of foreign atoms is much smaller than the concentration of host atoms. Thus, the host reaches quasi-equilibrium with its interstitials and vacancies in a way that is largely independent of what the foreign atoms do. This quasi-equilibrium implies that C_I, C_V, and C_H are essentially constant, and can be incorporated into pseudo first-order rate constants. Note that Cowern et al.[3] give similar expressions to those shown here with g and r in that treatment corresponding to K_{gen} and K_{ann}, respectively.

With the rate expressions given in Table 1, the governing equations for foreign atoms are given by

$$\partial C_M/\partial t = D_M \nabla^2 C_M - K_{ann}C_M + K_{gen}C_S \tag{1}$$

$$\partial (C_S + C_M)/\partial t = D_M \nabla^2 C_M \tag{2}$$

where D_M denotes the diffusivity of the mobile species. By hypothesis, mobile foreign atoms M exist in much smaller concentrations than substitutional atoms S, and can be considered as unstable intermediates in a chemical reaction. The classical quasi-steady state approximation can then be applied to M, implying that $\partial C_M/\partial t \approx 0$ Eqs. 1 and 2 can then be solved to yield the following analytical expression for C_S

$$C_S(x, t) = C_{\min} + (C_{\max} - C_{\min})s(\xi, \theta) \tag{3}$$

where C_{min} and C_{max} denote the initial and final concentration of foreign atoms in the step, and $s(\xi, \theta)$ is the normalized concentration. The variables $\xi = x/\lambda$ and $\theta = K_{gen}t$ respectively denote nondimensionalized space and time. The quantity θ equals the mean number ($\tilde{n}$) of migration steps (or equivalently, lattice exchanges) of the foreign atoms, and $\lambda = \sqrt{D_M/K_{ann}}$ equals the mean path length between the generation and annihilation events. The function $s(\xi, \theta)$ is then given by the following series expressions

$$s(\xi, \theta) = \sum_{n=0}^{\infty} P_n(\theta) f_n(\xi) \tag{4}$$

where

$$P_n(\theta) = (\theta^n/n!)e^{-\theta} \tag{5}$$

$$f_{n=0}(\xi) = H(\xi) \tag{6}$$

$$f_{n>0}(\xi) = \frac{1}{2^{2n-1}} \sum_{k=0}^{n-1} 2^k B_{n-1}^{2n-2-k} \left(2 - e^{-\xi} \sum_{l=0}^{k} \xi^l/l! \right) \quad \text{if } \xi > 0 \tag{7}$$

$$f_{n>0}(\xi) = \frac{1}{2^{2n-1}} \sum_{k=0}^{n-1} 2^k B_{n-1}^{2n-2-k} \left(e^{\xi} \sum_{l=0}^{k} (-\xi)^l/l! \right) \quad \text{if } \xi \le 0 \tag{8}$$

$H(\xi)$ represents the Heaviside step function, and B the binomial coefficient given by $B_k^n = n!/k!(n - k)!$. $P_n(\theta)$ gives the probability that a diffusing atom has exchanged with the lattice n times in time t, and $f_n(\xi)$ gives the spatial distribution of the migrated atoms. For short times with $\theta \ll 1$, the higher order terms in Eq. 4 can be neglected, leading to a first-order approximation incorporating only the terms $n = 0$ and $n = 1$

$$s(\xi, \theta) = e^{-\theta}\left(1 + \frac{\theta}{2}(2 - e^{-\xi})\right) \quad \text{if } \xi > 0 \tag{9}$$

$$s(\xi, \theta) = \theta e^{-\theta} e^{\xi}/2 \quad \text{if } \xi \le 0 \tag{10}$$

Equations 9 and 10 indicate that in this limit, the normalized foreign atom profile spreads with an exponential shape. However, since the amount of material that diffuses remains very small, significant deviations from the initial profile can be easily seen only on the depleted side of the step, where the large dynamic range of SIMS can be used to advantage. Equation 10 mirrors the expression derived by Cowern et al. for the case of an initial delta function profile. As time increases, the higher order terms in Eq. 4 become significant and cannot be neglected. When θ (and $\tilde{n}$) becomes large, the diffusion profile approaches an error function.

Figure 1 shows example profiles calculated from Eqs. 3 – 10 for various values of θ. For small values of θ, even the raw concentration profiles approximate an exponential shape near the initial step. Figure 2 shows the corresponding normalized concentrations s against x. In these plots, the true exponential shape shows clearly.

Figure 2 illustrates an additional useful feature of the step profile in the short-time limit when $\theta \ll 1$. The exponential tail breaks away sharply from the rest of the initial step at a normalized concentration s that is easily measured. The sharp break represents a true discontinuity in slope, and is the manifestation of a certain discretization in the system at very short times. Foreign atoms have moved either once or not at all, since $\tilde{n} \ll 1$. Atoms that have not moved at all remain fixed in the initial step, while those that have, show up in the exponential tail. The slope of the exponential tail on a semilogarithmic plot together with the breakaway concentration at $x = 0$ can be used to estimate θ and λ independently. Eqs. 2 and 10 can be written as

$$\ln\left(\frac{C_S(\xi, \theta) - C_{\min}}{C_{\max} - C_{\min}}\right) = \ln(s(\xi, \theta)) = \frac{\theta}{2} e^{\xi} \qquad (11)$$

or alternatively

$$\ln\left(\frac{C_S(x, t) - C_{\min}}{C_{\max} - C_{\min}}\right) = \ln(s(x, t)) = \ln(K_{gen}t/2) + x/\lambda \quad (12)$$

Thus, plotting the normalized concentration s against x at a particular time t yields a straight line giving λ and K_{gen} from the slope and intercept, respectively.

This approach has advantages over the delta function method. Note that λ and K_{gen} are determined completely independently in Eq. 12. In the delta function method, K_{gen} is determined from the width of the diffused profile, which equals $\lambda\sqrt{2K_{gen}t}$.[3] Thus, errors in λ propagate directly into errors in K_{gen}. In addition, the standard deviation approach suffers when the initial profile contains some pre-existing broadening. Deposition methods often induce this broadening because of diffusion during growth (which is symmetric about the $x = 0$ point for the step and delta function), or nonidealities in how the flux of foreign atoms is started or stopped (which may not be symmetric about $x = 0$). Convolution of the series solution for the delta function case with the initial profile shape is needed to determine the change in standard deviation due to diffusion.[3] This procedure can also be used for the step function case, but the intercept can also be determined more simply from the discontinuity in slope that is present even when the initial profile is broadened. Of course, some error is entailed in this procedure, because the diffusing species now originate from a region in the profile where the concentration is less than C_o. However, for the profiles measured experimentally here, the error is no more than 10 – 15% in the computed parameters compared to a full numerical solution. Since the reproducibility of the experiment is at least of this order, the error of using the intercept approach is not especially significant.

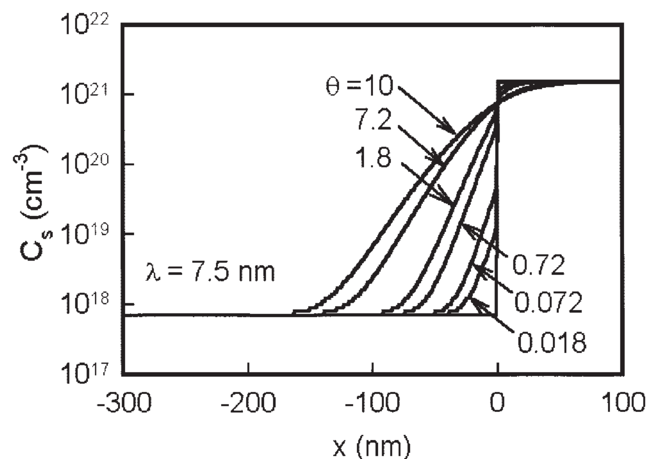

Figure 1. Simulated profiles for dopant diffusion for various values of θ.

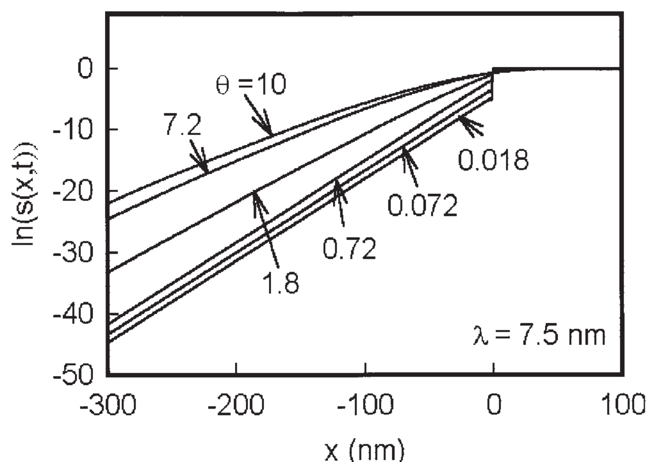

Figure 2. Normalized concentrations s corresponding to the data in Figure 1.

The straight lines for small values of θ reflect the "exponential tails."

Experiment

Self-diffusion of silicon provides a convenient test case for the expressions derived above. Other groups have examined long-time diffusion of ^{30}Si from substrates with natural isotopic abundances into epitaxially grown layers depleted in ^{30}Si.[1,14,15] The natural isotope abundances in Si are 92.2% mass 28, 4.7% mass 29, and 3.1% mass 30. The epitaxial layers are grown by low-pressure chemical vapor deposition atop the natural-abundance substrates, and the concentration of ^{30}Si within the layers typically lays three orders of magnitude below the natural level. Diffusion measurements then track the spreading of the step concentration profile of ^{30}Si within the isotopic heterostructure. We applied a similar experimental design to short-time diffusion, except that our annealing was performed in ultrahigh vacuum.

Step-function isotope structures were obtained as 4-in. n-doped wafers from Isonics Corporation. Arsenic served as the dopant, and was present at a uniform level throughout the step function structure at a concentration of 1×10^{19} cm^{-3}. The concentration of ^{30}Si within the grown layer was 0.002%. Specimens of approximate dimensions 1.3 cm×0.5 cm were

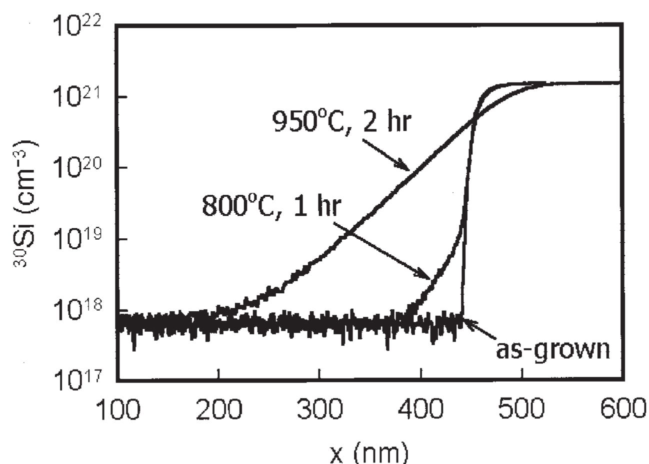

Figure 3. Experimental ^{30}Si diffusion profiles after annealing.

cut from the wafers and degreased by successive 5-min rinsing cycles in electronic-grade trichloroethylene, acetone, and methanol. Native oxide was removed with 49% HF followed by rinsing in deionized water for 1 min. Immediately thereafter, a typical specimen was mounted for resistive heating by clamping against a thin Ta foil using Ta clips, and then placed in a turbomolecularly pumped ultrahigh vacuum chamber that was quickly pumped down to 10^{-9} torr to avoid significant native oxide formation. Temperature was monitored with a chromel-alumel thermocouple spot welded to the Ta foil adjacent to the edge of the Si specimen.

Heating the structure to above 600°C led to silicidation of the Si/Ta interface (without significant diffusion of the isotope), promoting good thermal and electrical contact. Further annealing to induce profile spreading took place above 800°C. Isotope profiles were measured *ex situ* with secondary ion mass spectroscopy (SIMS) using a CAMECA IMS-5f instrument with a cesium ion beam. Multiple SIMS measurements were made for each specimen to improve the accuracy of parameter determination.

Results and Discussion

Figure 3 shows typical diffused ^{30}Si profiles obtained at two different annealing temperatures and times. The exponential shape for small diffusion lengths and the error-function shape at larger lengths are evident. The initial profile exhibited nontrivial spreading in the as-received wafers. Hence, to obtain the parameters λ and θ, a nonlinear least-squares fitting routine was employed together with direct solution of Eqs. 1 and 2 using a differential equation solver. The effective diffusivity D_{eff} was calculated from the relation[4]

$$D_{eff} = K_{gen}\lambda^2 \tag{13}$$

At long diffusion times, fitting the profiles with the conventional error function expression gave values of D_{eff} differing by only 1-2% from those calculated by Eq. 13. Table 2 lists the fitting parameters and the diffusivities calculated using Eq. (13) for the two temperatures. For a 95% confidence interval, the errors in θ, λ and D_{eff} are 5%, 2% and 10%, respectively.

The exponential shape of the short-distance profile in Figure 3 gives clear evidence of a mechanism involving a highly mobile intermediate species. A simple vacancy mechanism cannot account for this shape because the diffusing atom does not go into a highly mobile state. A vacancy pairing mechanism outlined in Table 1 can explain the data in principle, but seems unlikely in the case of Si self-diffusion because there is no mechanism for such pairing. Such a mechanism has been postulated for diffusion of dopants in Si, where interaction between the vacancy and dopant atom arises from coulombic attraction[7] or possibly short-range elastic forces.[7] However, both of these interactions require that the foreign atom differs chemically from the host so that charging and/or lattice distortion can take place. Such effects do not occur when the foreign atoms are merely labeled isotopically. The data of Figure 3 cannot distinguish between interstitial mechanisms involving vacancy-interstitial (or "Frank-Turnbull") dissociation as opposed to kickout, as has been proven by Marioton et al.[9] and Cowern.[2] Such a distinction requires variation of point defect concentrations in a controlled manner as outlined by Cowern et al.[4]

The diffusivities shown in Table 2 are two to four orders of magnitude larger than typical diffusivities reported in literature at similar temperatures.[7,8,11] It is well known that self-diffusion measurements in Si suffer from large but unexplained discrepancies among laboratories.[7,8,11] We will discuss the likely reasons for these differences elsewhere.[5] Note, however, that the large diffusivities reported here do not arise from the mathematical framework for analysis; standard error function fitting at long times yields essentially the same results as the more complicated equations derived here.

Conclusion

The diffusion method developed here for initial step profiles shares the advantages of related methods already described for delta functions, but offers the additional advantages of fabrication ease and analytical ease in the short-time limit. In the particular case of Si self-diffusion, exponential tails on short-time profiles give clear evidence that interstitials mediate the dynamics under the conditions of the experiments.

Acknowledgments

This work was partially supported by NSF (CTS 02-03237). SIMS was performed at the Center for Microanalysis of Materials in the Frederick Seitz Materials Research Laboratory at the University of Illinois, which is partially supported by the U.S. Dept. of Energy under grant DEFG02-96-ER45439. We thank Judith Baker for significant help in interpreting the

Table 2. Measured Diffusion Parameters

Diffusion Temperature (°C)	Annealing Time (hr)	θ	λ (nm)	K_{gen} (s^{-1})	D_{eff} (cm^2/s)
800	1	0.3	7.0	8.5×10^{-5}	4.2×10^{-17}
950	2	47	5.5	6.5×10^{-3}	2.0×10^{-15}

SIMS results, and Steve Burdin at Isonics Corp for overseeing the successful creation of isotopically labeled specimens.

Literature Cited

1. Bracht H, Haller EE, Clark-Phelps R. Silicon self-diffusion in isotope heterostructures. *Phys Rev Lett.* 1998;81:393-396.
2. Cowern NEB. General model for intrinsic dopant diffusion in silicon under nonequilibrium point-defect conditions. *J Appl Phys.* 1988;64: 4484-4490.
3. Cowern NEB, Jansen KTF, van de Walle GFA, Gravesteijen DJ. Impurity Diffusion via an Intermediate species: The B-Si System. *Phys Rev Lett.* 1990;65,2434-2437.
4. Cowern NEB, van de Walle GFA, Gravesteijen DJ, Vriezema CJ. Experiments on Atomic-Scale Mechanisms of Diffusion. *Phys Rev Lett.* 1991;67,212-215.
5. Dev K, Vaidyanathan R, Jung MYL, Braatz RD, Seebauer EG. to be published.
6. Fahey PM, Griffin PB, Plummer JD. Point defects and dopant diffusion in silicon. *Rev Mod Phys.* 1989;61:289-384.
7. Fair RB. In: *Silicon Integrated Circuits.* Part B. edited by Kahng D. New York: Academic Press; 1981:1.
8. Frank W, Goesele U, Mehrer H, Seeger A. In: *Diffusion in Crystalline Solids.* edited by Murch GE, Nowick AS. New York: Academic Press; 1984.
9. Marioton BPR, Goesele U, Tan TY. Self-interstitials required to explain nonequilibrium diffusion phenomena in silicon. *Chemtronics.* 1986;1:156.
10. Nichols CS, van de Walle CG, Pantelides ST. Mechanisms of Equilibrium and Nonequilibrium Diffusion of Dopants in Silicon. *Phys Rev Lett.* 1989;62:1049-1052.
11. Sharma BL. Diffusion in silicon and germanium. In: *Defect and Diffusion Forum.* 1990;70-71:1.
12. Shewmon P. *Diffusion in Solids*. Warrendale, PA: Minerals, Metals & Materials Soc; 1989.
13. Ural A, Griffin PB, Plummer JD. Fractional contributions of microscopic diffusion mechanisms for common dopants and self-diffusion in silicon. *J Appl Phys*. 1999;85:6440-6446.
14. Ural A, Griffin PB, Plummer JD. Self-diffusion in silicon: similarity between the properties of native point defects. *Phys Rev Lett.* 1999; 83:3454-3457.
15. Ural A, Griffin PB, Plummer JD.Nonequilibrium experiments on self-diffusion in silicon at low temperatures using isotopically enriched structures. *Physica B.* 1999;273-274:512-515.

Manuscript received Feb. 11, 2005, and revision received Apr. 29, 2005.